

DOCUMENT CONTROL SHEET

	ORIGINATOR'S REF. NLR TP 96036 U		SECURITY CLASS. Unclassified																		
ORIGINATOR National Aerospace Laboratory NLR, Amsterdam, The Netherlands																					
TITLE Development of a fully automated CFD system for three-dimensional flow simulations based on hybrid prismatic-tetrahedral grids																					
PRESENTED AT the 5th International Conference on Numerical Grid Generation in Computational Fluid Dynamics and related fields, Starkville, Mississippi, April 1996																					
AUTHORS J.W. van der Burg, J.E.J. Maseland and B. Oskam		DATE 960117	pp ref 17 29																		
DESCRIPTORS <table style="width: 100%; border: none;"> <tr> <td style="width: 33%;">Adaptation</td> <td style="width: 33%;">Computer aided design</td> <td style="width: 33%;">Turbulence models</td> </tr> <tr> <td>Algorithms</td> <td>Navier-Stokes equation</td> <td></td> </tr> <tr> <td>Body-wing configurations</td> <td>Prisms</td> <td></td> </tr> <tr> <td>Computational fluid dynamics</td> <td>Tetrahedrons</td> <td></td> </tr> <tr> <td>Computational geometry</td> <td>Three dimensional models</td> <td></td> </tr> <tr> <td>Computational grids</td> <td>Triangulation</td> <td></td> </tr> </table>				Adaptation	Computer aided design	Turbulence models	Algorithms	Navier-Stokes equation		Body-wing configurations	Prisms		Computational fluid dynamics	Tetrahedrons		Computational geometry	Three dimensional models		Computational grids	Triangulation	
Adaptation	Computer aided design	Turbulence models																			
Algorithms	Navier-Stokes equation																				
Body-wing configurations	Prisms																				
Computational fluid dynamics	Tetrahedrons																				
Computational geometry	Three dimensional models																				
Computational grids	Triangulation																				
ABSTRACT In this paper an assessment of CFD methods based on the underlying grid type is made. It is safe to say that emerging CFD methods based on hybrid body-fitted grids of tetrahedral and prismatic cells using unstructured data storage schemes have the potential to satisfy the basic requirements of problem-turnaround-time and accuracy for complex geometries. The CFD system described in this paper is based on the hybrid prismatic-tetrahedral grid approach. In an analysis it is shown that the cells in the prismatic layer have to satisfy a central symmetry property in order to obtain a second-order accurate approximation of the viscous terms in the Reynolds-averaged Navier-Stokes equations. Prismatic grid generation is demonstrated for the ONERA M6 wing-alone configuration and the AS28G wing/body configuration.																					

NLR TECHNICAL PUBLICATION

TP 96036 U




DEVELOPMENT OF A FULLY AUTOMATED CFD SYSTEM  
FOR THREE-DIMENSIONAL FLOW SIMULATIONS BASED ON  
HYBRID PRISMATIC-TETRAHEDRAL GRIDS


by

J.W. van der Burg, J.E.J. Maseland and B. Oskam

This paper is presented at the 5th International Conference on Numerical Grid Generation in Computational Fluid Dynamics and related fields, Starkville, Mississippi, April 1996.

Division : Aerodynamics

Prepared : JWvdB/  JEJM/  BO/ 

Approved : JWS/ 

Completed : 960117

Order number : 526.303

Typ. : JWvdB/MM



## **Abstract**

In this paper an assessment of CFD methods based on the underlying grid type is made. It is safe to say that emerging CFD methods based on hybrid body-fitted grids of tetrahedral and prismatic cells using unstructured data storage schemes have the potential to satisfy the basic requirements of problem-turnaround-time and accuracy for complex geometries. The CFD system described in this paper is based on the hybrid prismatic-tetrahedral grid approach. In an analysis it is shown that the cells in the prismatic layer have to satisfy a central symmetry property in order to obtain a second-order accurate approximation of the viscous terms in the Reynolds-averaged Navier-Stokes equations. Prismatic grid generation is demonstrated for the ONERA M6 wing-alone configuration and the AS28G wing/body configuration.



## Contents

<b>1</b>	<b>Introduction</b>	<b>5</b>
<b>2</b>	<b>Assessment of CFD-systems</b>	<b>6</b>
<b>3</b>	<b>Overview of the CFD system</b>	<b>7</b>
3.1	Surface triangulation algorithm	7
3.2	Three-dimensional hybrid prismatic-tetrahedral grid generation	7
3.3	Pre-processing algorithm	8
2.4	Flow calculation	8
3.5	Grid adaption	8
<b>4</b>	<b>Three-dimensional prismatic grid generation</b>	<b>9</b>
4.1	Central symmetry property for prismatic grid	9
4.2	Applications of prismatic grid generation algorithm	10
<b>5</b>	<b>Conclusions</b>	<b>12</b>
<b>6</b>	<b>References</b>	<b>13</b>

1 Table

6 Figures

(17 pages in total)

## 1 Introduction

The European aerospace industry faces a multitude of crucial business and industrial challenges if it is to respond effectively to market opportunities arising from the continuous growth in demand for air transport. Reduced costs and faster aircraft development cycles are critical factors for competitive advantage in the changing world of airplane design (Ref. 1). Aerospace industry needs in CFD technology as derived from these critical factors for new commercial transport aircraft, can be formulated in terms of requirements to be satisfied by CFD codes and supercomputers. For CFD technology to have an impact on the aerodynamic design of airplanes the first requirement to be satisfied is that the CFD-problem-turnaround-time (incl. grid generation) must be in the order of a day to a week, or less. Aerodynamic analysis is a process of looking at a significant number of flow conditions (lift coefficients, Mach numbers, Reynolds numbers) for more than one geometric variant such that a large number of calculations have to be made. If the application of CFD codes does not yield results at this industrial time scale the impact on aerodynamic design will be reduced (Ref. 1). A second requirement which needs to be met by CFD tools for the development of commercial transport aircraft is high accuracy of predicted aerodynamic forces such that computed drag, pitching moment and lift can be relied upon to reduce the risks involved in airplane design. This second requirement translates for example into better turbulence models, and extreme grid resolution or automatic, adaptive grid generation if the first requirement (CFD-problem-turnaround-time) is also to be satisfied simultaneously.

The objective of the present research is focussed on the development of an automatic CFD system based on Reynolds-averaged Navier-Stokes equations applicable to complete aircraft configurations e.g. aircraft with engines and high lift systems.

## 2 Assessment of CFD-systems

A review of the open literature on CFD flow solvers, as discussed in (Ref. 2), provides a list of CFD flow solvers based on multi-block, tetrahedral or hexahedral approaches currently employed in aerospace companies, research establishments and universities both in US and Europe (see Table 1). It can be observed that a large number of existing multi-block based CFD-systems have approximately the same technical basis. The current status of the multi-block method (type 1) is characterised by the observation that the method is the most widely used approach for civil transport design, and that it is in use for turbulent compressible Navier-Stokes. Due to the fact that grid generation is not automatic, CFD-systems based on regular body-fitted grids (type 1) and irregular body-fitted grids of hexahedra (type 3) are not acceptable with respect to turnaround time. At present for the gridless grid approach (type 7) a three-dimensional multi-block-type grid is required as input.

For CFD-systems based on the tetrahedral grid approach (type 2), the accuracy of the predictions obtained with such a CFD-system is degraded due to cross-wind diffusion although grid generation is fully automatic (even for complex geometries). The Chimera approach (type 5) has not been demonstrated yet for complex aircraft configurations without sacrificing either computational efficiency or accuracy in the overlapping parts. For Cartesian embedded grids (type 6) Navier-Stokes calculations are not feasible.

The use of the hybrid grid approach (type 4) in the CFD-system combines the advantages of the unstructured tetrahedral approach (type 2) and the regular body-fitted grids (type 1) (Ref. 19). A high accuracy of predictions is obtained by generating a regular structure of prismatic cells near solid boundaries of the computational domain and tetrahedral elements in the inviscid part of the flow domain. Due to the fact that generation of a surface grid (with triangular elements) and the three-dimensional grid generation (prismatic and tetrahedral part) are automatic even for very complex geometries the problem-turnaround-time can be reduced significantly.

### 3 Overview of the CFD system

The CFD-system based on the hybrid grid approach contains the algorithmic components shown in Figure 1. The starting point of the CFD system is the geometry of an aircraft configuration which is usually defined in terms of a standard CAD data format constructed using a CAD system e.g. ICEM-CFD (ICEM=Integrated Computer-aided Engineering and Manufacturing). To make the geometry suited for flow simulations a closed aerodynamic surface has to be defined. This means that overlapping surfaces and gaps and holes in the geometry have to be removed. This can be a time-consuming process. Afterwards a topologically Cartesian grids is generated on these surfaces using a CAD system which can be time-consuming for complex aircraft configurations.

#### 3.1 Surface triangulation algorithm

In view of the required reduction of total turnaround time the surface triangulation algorithm interfaces directly to the CAD system thereby by-passing the user generation of Cartesian grids. The exchange of geometrical data is in a standard CAD data format:

1. IGES: International Graphics Exchange Standard (Ref. 20).
2. VDA-FS: Verband der Automobilindustrie-Flächen Schnittstelle (Refs. 21, 22).
3. STEP: STandard for the Exchange of Product model data (Ref. 23).

These data formats can be obtained from the CATIA data format using a commercially available interface.

Typically, the geometry of the aerodynamic surface is established in terms of geometric entities, viz. curves and surfaces. The relation between these geometric entities, referred to as the topology, has to be defined explicitly. The curves and surfaces are modelled by means of higher order polynomials.

#### 3.2 Three-dimensional hybrid prismatic-tetrahedral grid generation

The generation of a hybrid grid consisting of prismatic and tetrahedral elements starts with the generation of prismatic cells near solid walls of the flow domain.

The prismatic cells are constructed by advancing the nodes on the triangulated geometry into the computational flow domain along marching vectors associated to the nodes. In every advancing step, a whole layer of prismatic elements is created and therefore this approach is termed as the advancing layer approach.

By adding the far field boundaries and a symmetry plane (optional) to the grid marching surface of the prismatic grid, a bounded flow domain is defined in which inviscid flow is assumed. The geometry of the far field boundaries and the symmetry plane is discretized using the surface triangulation algorithm of the previous section. Subsequently, a tetrahedral grid of Delaunay-

type is generated in the inviscid flow domain by employing a three-dimensional grid generation algorithm (Ref. 24).

Finally, the nodes on the intersecting surface between the prismatic grid and the tetrahedral grid are merged and the hybrid grid generation process is concluded.

### **3.3 Pre-processing algorithm**

To achieve a high level of performance of the flow calculation algorithm on a vector and parallel computer architecture like the NEC SX4 a pre-processing algorithm has to be employed for the generated three-dimensional hybrid grid. Usage of an unstructured hybrid grid results in extensive use of indirect addressing. As in the flow calculation algorithm (next algorithmic step) an edge-based data structure is utilised, a colouring algorithm for the edges in the hybrid grid is employed to avoid vector dependencies. A partitioning algorithm is employed to decompose the three-dimensional hybrid grid. This supports parallelisation of the flow calculation algorithm.

### **3.4 Flow calculation**

In the flow calculation algorithm three-dimensional viscous flow is simulated. To this purpose the time-accurate three-dimensional Reynolds-averaged Navier-Stokes equations are marched in time towards steady state by a Runge-Kutta time stepping method. Local time stepping, residual averaging and multigrid are used to accelerate convergence. An edge-based data structure is employed which results in a flow solver which is optimised in terms of computer memory requirements and computational performance.

### **3.5 Grid adaption**

Hybrid grid adaption algorithm is based on remeshing. Based on values of an residual based indicator (Ref. 25) the surface triangulation of the aerodynamic surface is adapted. The nodes are placed on the actual geometry description as defined by the CAD data format.

The prismatic grid is directionally refined in normal direction to the aerodynamic surface (Ref. 12). This means that for each newly generated node on the triangulated aerodynamic surface a new node is introduced in the prismatic front.

The far field boundaries and the symmetry plane are refined by node insertion and finally the three-dimensional grid generation algorithm is adopted to generate an entirely new three-dimensional hybrid grid. By incorporating the newly generated source terms in the existing distribution function a locally refined grid is obtained. For the adapted grid a numerical solution is then obtained by first employing the pre-processing algorithm and subsequently the flow calculation algorithm. This process (see Figure 1) is repeated until a numerical solution of sufficient accuracy is obtained. The adapted grids will show an enhanced definition of flow features e.g. shocks and slip lines.



## 4 Three-dimensional prismatic grid generation

The prismatic grid generation algorithm starts from a triangulated aerodynamic surface. The three-dimensional prismatic grid is created on this surface by advancing the triangulated surface in normal direction over a specified distance. In order to accurately simulate viscous flows on a hybrid grid the prismatic grid is required to satisfy a central symmetry property (see references (Refs. 19, 26)). It is shown here that the central symmetry property yields a second-order accurate discretisation for a diffusive term on a prismatic grid.

### 4.1 Central symmetry property for prismatic grid

On the wing surface the diffusion in normal direction is large compared to the diffusion in tangential direction, leading to highly stretched grids (in normal direction) for large Reynolds numbers. On this location of the wing surface a grid containing prismatic elements is generated.

Consider the volume integral of the Laplace operator

$$\int \int \int_{\Omega} \text{div}(\nabla u) dV = \int \int_{\partial\Omega} (\mathbf{n}, \nabla u) dS, \quad (1)$$

where  $\nabla = [\partial/\partial x, \partial/\partial y, \partial/\partial z]^T$  denotes the gradient operator and  $\Omega$  is a control volume located in the flow domain. Gauss theorem yields a surface integral where  $\mathbf{n}$  is the normal vector to the control volume.

By employing a finite volume method using a vertex-based control volume for the prismatic cells surrounding central node  $j$  (see Figure 2) the surface integral is written as

$$\sum_i \int \int_{\partial\Omega_i} (\mathbf{n}_i, \nabla u) dS,$$

where  $\mathbf{n}_i = [n_{i1}, n_{i2}, n_{i3}]^T$  is the unit normal vector to surface  $\partial\Omega_i$  of the vertex-based control volume (see Figure 3). The value of the gradient on the surface  $\partial\Omega_i$  is determined by linear interpolation (Refs. 27, 28) as

$$\sum_i S_i (\mathbf{n}_i, \frac{\nabla u_i + \nabla u_j}{2}), \quad (2)$$

where  $j$  is the central node and  $S_i$  is the surface area of  $\partial\Omega_i$ .

A Taylor expansion around the central node yields

$$\nabla u_i = \nabla u_j + \nabla(\mathbf{h}_i, \nabla u) + \frac{1}{2} \nabla(\mathbf{h}_i, \nabla(\mathbf{h}_i, \nabla u)) + \mathcal{O}(\|\mathbf{h}_i\|^3),$$

with  $\mathbf{h}_i = [x_i - x_j, y_i - y_j, z_i - z_j]^T$ . By substituting this relation in (2) the discretisation error for approximating (1) is obtained

$$\sum_i S_i(\mathbf{n}_i, \frac{1}{2}\nabla(\mathbf{h}_i, \nabla(\mathbf{h}_i, \nabla u))) \quad (3)$$

As diffusion in normal direction is dominant, the terms significantly contributing to the discretisation error are

$$\begin{aligned} E_1 &= \sum_i \frac{1}{2} S_i n_{i1} (x_i - x_j) (z_i - z_j) \frac{\partial^3 u}{\partial x \partial z^2}, \\ E_2 &= \sum_i \frac{1}{2} S_i n_{i2} (y_i - y_j) (z_i - z_j) \frac{\partial^3 u}{\partial y \partial z^2}, \\ E_3 &= \sum_i \frac{1}{2} S_i n_{i3} (z_i - z_j)^2 \frac{\partial^3 u}{\partial z^3}. \end{aligned}$$

These error terms vanish in case

1. The triangulated surface in which node  $j$  is contained is planar, which means that  $z_i - z_j = 0$  for nodes in this triangulation.
2. The unit normal vectors  $\mathbf{n}_1$  and  $\mathbf{n}_2$  corresponding to the surfaces  $\partial\Omega_1$  and  $\partial\Omega_2$  of the control volume are opposite and the associated surface areas are identical  $S_1 = S_2$ .
3. The nodes  $\mathbf{x}_1$  and  $\mathbf{x}_2$  are located centrally symmetric around node  $j$

$$\begin{aligned} x_2 - x_j &= -(x_1 - x_j), \\ y_2 - y_j &= -(y_1 - y_j), \\ z_2 - z_j &= -(z_1 - z_j). \end{aligned}$$

In such a way the Laplacian operator (1) is discretised with second-order accuracy in normal direction to the wing surface.

Due to the fact that in viscous flow simulations diffusion in normal direction to the wing surface is large compared to diffusion in tangential direction it is required that the step size in normal direction, expressed by  $z_1 - z_j$ , is small compared to the tangential direction. This results in a prismatic grid with high aspect ratio cells.

#### 4.2 Applications of prismatic grid generation algorithm

The prismatic grid generation algorithm starts with the construction of surface normals at each node on the advancing surface. A surface normal vector  $\vec{n}_j$  and a visibility half-cone angle  $\beta_j$  is



associated to node  $j$  following a modified approach of Kallinderis (Ref. 11). Our approach constructs good surface normals at nodes located on sharp edges or combined acute/obtuse geometry junctions. The parameter  $\beta_j$  permits the user to control the degree of orthogonality of the grid lines by restricting the value for  $\beta$ . The surface normals  $\vec{n}_j$  defines the initial marching vectors  $\vec{m}_j$ . Advancement of the nodes in the initial marching directions may possibly lead to prismatic cells with overlapped faces. Therefore, the marching vectors are smoothed such that a smooth grid is obtained without overlapping. Smoothing of both marching vector and marching step is achieved by a point-wise minimization technique which distributes points equally spaced on each marching surface and reduces the marching surface curvature.

In Figure 4 a close-up of an Euler-type hybrid grid around the ONERA M6 wing is shown. Refinement of the wing leading, trailing edge and wing tip was necessary in order to obtain prismatic cells with a desirable shape. In the prismatic layer 10 cells in normal direction to the wing surface are generated. In the smoothing algorithm 30 smoothing steps are taken. Figure 5 contains an Euler solution calculated on the hybrid grid for ONERA M6 wing. In Figure 6 an example of a hybrid grid around the AS28G wing/body configuration (see also reference (Ref. 29)) is shown.

## 5 Conclusions

The hybrid prismatic-tetrahedral grid approach is chosen to develop a CFD system for three-dimensional flows which has a very short problem-turnaround-time and which yields a high accuracy of aerodynamic entities. Grid adaption based on remeshing is incorporated to predict flow features more accurately.

It is shown that the cells in the prismatic grid on the wing surface have to satisfy a central symmetry property in order to obtain an accurate approximation of diffusive terms appearing in the Reynolds-averaged Navier-Stokes equations.

Hybrid grid generation is demonstrated for the ONERA M6 wing alone and the AS28G wing/body configuration. For the ONERAM6 wing alone configuration a flow solution is obtained on a hybrid grid.

## Acknowledgements

The three-dimensional Euler solution on the hybrid grid that is shown in Figure 5 is generated by O. Friedrich of DLR within the framework of the DLR/NLR cooperation "CFD for Complete Aircraft"



## 6 References

1. Rubbert, P.E., CFD and the changing world of airplane design, In *ICAS Proceedings, 19th Congress of the International Council of the Aeronautical Sciences*, September 1994.
2. Computational aerodynamics based on the Euler equations, AGARDograph AGARD-AG-325, 1994.
3. Frink, N.T., Pirzadeh S., An unstructured-grid software system for solving complex aerodynamic problems, Proceedings of the NASA workshop on Surface Modeling, Grid Generation and related issues in CFD solutions, Cleveland, Ohio, May 1995.
4. Hassan, O., Probert, E.J., Weatherill, N.P., Marchant, M.J., Morgan, K., Marcum, D.L., The numerical simulation of viscous transonic flow using unstructured grids, AIAA-94-2346, 1994.
5. Löhner R., Matching semi-structured and unstructured grid for Navier-Stokes calculations, AIAA-93-3348-CP, 1993.
6. Marchant, M.J., Weatherill, N.P. Unstructured grid generation for viscous flow simulations, In Weatherill, N.P., Eiseman, P.R., Häuser, J., Thompson, J.F., editor, *Numerical grid generation in Computational Fluid Dynamics and related fields*, 1994.
7. Mavripilis, D.J., A Three-dimensional multigrid Reynolds-averaged Navier-Stokes solver for unstructured meshes, ICASE report 94-29, 1994.
8. Pirzadeh, S., Viscous unstructured three-dimensional grid by the advancing layers method, AIAA-94-0417, 1994.
9. Aftosmis, M.J., An upwind method for the solution of the 3D Euler and Navier-Stokes equations on adaptively refined meshes, WL-TR-92-3107, 1992.
10. Aftosmis, M.J., Viscous flow simulation using an upwind method for hexahedral based adaptive meshes, AIAA 93-0772, 1993.
11. Kallinderis, Y., Khawaja, A., McMorris, H., Adaptive hybrid prismatic-tetrahedral grids for viscous flows, Proceedings of the NASA workshop on Surface Modeling, Grid Generation and related issues in CFD solutions, Cleveland, Ohio, May 1995.
12. Minyard, T., Kallinderis, A parallel Navier-Stokes method and grid adapter with hybrid prismatic/tetrahedral meshes, AIAA 95-0222, Reno, Nevada, 1995.
13. Parthasarathy, V., Kallinderis, Y., Nakajima, K., Hybrid adaptation method and directional viscous multigrid with prismatic-tetrahedral meshes, AIAA 95-0670, Reno, Nevada, 1995.
14. Benek, J.A., Buning, P.G., Steger J.L., A 3-D CHIMERA grid embedding technique, AIAA-85-1523, 1985.
15. Kao, K.H., Liou, M.S., Direct replacement of arbitrary grid-overlapping by nonstructured grid, AIAA-95-0346, 1995.



16. Chiu, I.T., Meakin, R., On automating domain connectivity for overset grids, AIAA-95-0854, 1995.
17. Melton, J.E., Berger, M.J., Aftosmis, M.J., Wong, M.D., 3D applications of a Cartesian grid Euler method, AIAA-95-0853, 1995.
18. Batina, J.T., A gridless Euler/Navier-Stokes solution algorithm for complex aircraft applications, AIAA-93-0333, 1993.
19. T.J. Baker, Prospects and expectations for unstructured methods, Proceedings of the NASA workshop on Surface Modeling, Grid Generation and related issues in CFD solutions, Cleveland, Ohio, May 1995.
20. IGES, Initial Graphics Exchange Specification (IGES) Version 1.0, US-department of Commerce, National Bureau of Standards, 1988.
21. VDA, Format for the exchange of geometric information (VDA/VDMA-FS), draft of the German standard DIN 66301, 1987.
22. VDA-Working Group CAD/CAM, VDA Surface data interface (VDAFS) version 2.0, 1987.
23. Shaw, N., Owen, J., *Outline of the integrated Product Information Model and Express*, CADDETC, 1988.
24. N.P. Weatherill, O. Hassan, D.L. Marcum, Calculation of steady compressible flow fields with the finite element method, AIAA-93-0341, 1993.
25. Th. Sonar, Strong and weak norm refinement indicators based on the finite element residual for compressible flow computations, *Impact of Computing in Science and Engineering* 5, 111-127, 1993.
26. P.L. Roe, Error estimates for cell-vertex solutions of the compressible Euler equations, NASA Contractor Report 178235, ICASE report No. 87-6, 1987.
27. T.J. Barth, Numerical aspects of computing viscous high Reynolds number flows on unstructured meshes, AIAA-91-0721, Reno, Nevada, January 1991.
28. M. Galle, Solution of the Euler- and Navier-Stokes equations on hybrid grids, AGARD F.D.P. Symposium on Progress and Challenges in CFD Methods and Algorithms, Seville, 2-5 October 1995.
29. J.W. van der Burg, J.E.J. Maseland, R. Hagmeijer, K.M.J. de Cock, Demonstration of an automated CFD system for three-dimensional flow simulations, Proceedings of the NASA workshop on Surface Modeling, Grid Generation and related issues in CFD solutions, Cleveland, Ohio, May 1995.

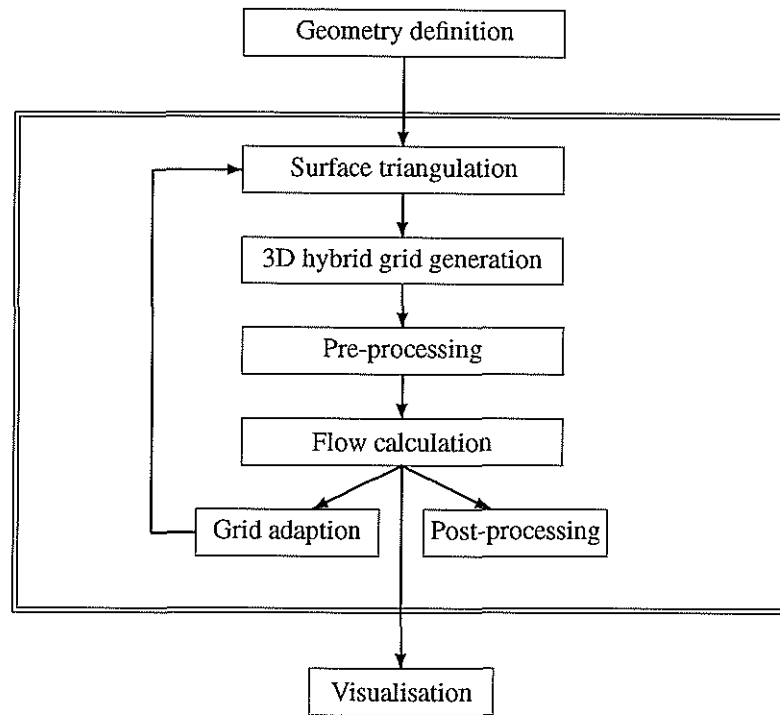


Fig. 1 Algorithmic components of the CFD-system

Grid type	Turnaround time	Ext. to N.S.	Accuracy for N.S.	References
1. Regular body-fitted grid of hexahedra	Not Acc.	Yes	Good	(Ref. 2)
2. Irregular body-fitted grid of tetrahedra	Good	No	Not Acc.	(Refs. 3, 4, 5) (Refs. 6, 7, 8)
3. Irregular body-fitted grid of hexahedra	Not Acc.	Yes	Good	(Refs. 9, 10)
4. Hybrid prismatic-tetrahedral grid	Good	Yes	Good	(Refs. 11, 12, 13)
5. Overlapping component-fitted Chimera	Not Acc.	Yes	Not eff.	(Refs. 14, 15, 16)
6. Cartesian embedded grids	Good	No	Not Acc.	(Ref. 17)
7. Gridless grid approach	Not Acc.	No	Not Acc.	(Ref. 18)

Table 1 Assessment of CFD-systems based on the different grid types; (Ext.=Extension; Not Acc.=Not Acceptable; Not eff.=Not efficient; N.S.= Navier-Stokes)

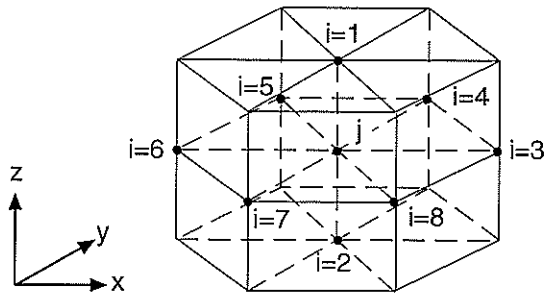


Fig. 2 Prismatic cells surrounding the central node  $j$

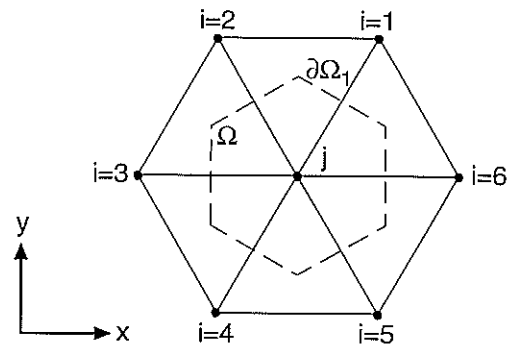


Fig. 3 Example of the vertex-based control volume in two dimensions

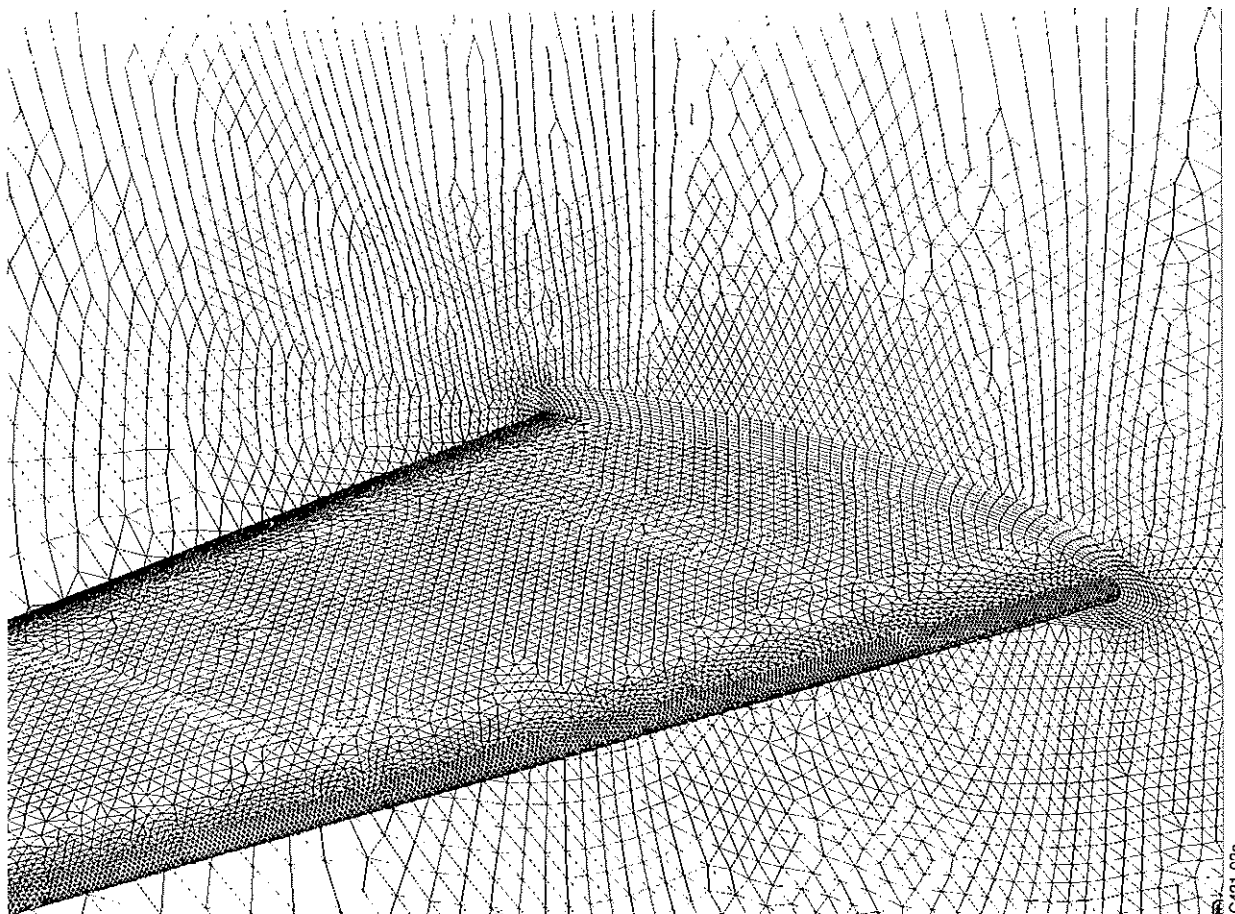
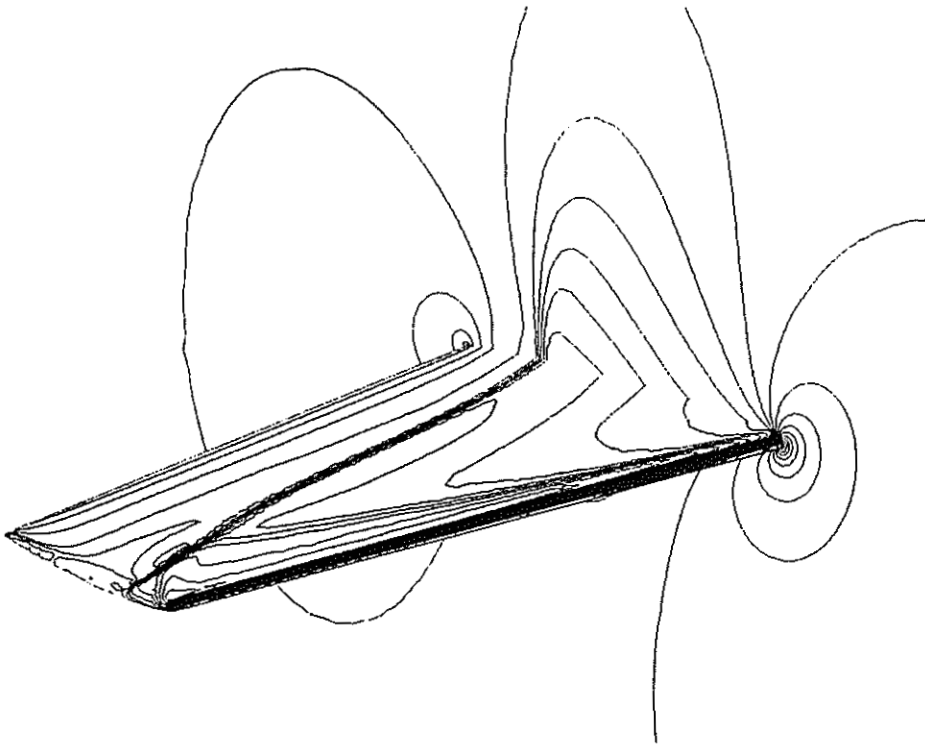
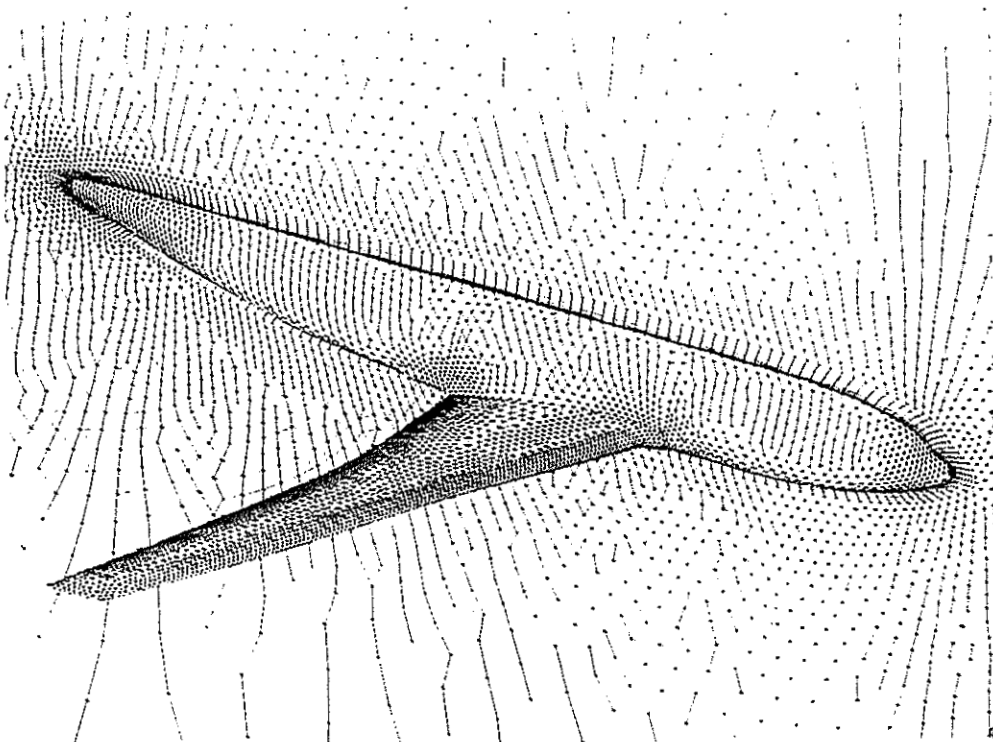


Fig. 4 Hybrid prismatic/tetrahedral grid around the ONERA M6 wing





*Fig. 5 Euler solution calculated on the hybrid (tetrahedral/prismatic) grid for the ONERA M6 wing*



*Fig. 6 Hybrid prismatic/tetrahedral grid around the AS28G wing/body configuration*